Initial Timing Acquisition for Binary Phase-Shift Keying Direct Sequence Ultra-wideband Transmission

Kyu-Min Kang and Sang-Sung Choi

This paper presents a parallel processing searcher structure for the initial synchronization of a direct sequence ultra-wideband (DS-UWB) system, which is suitable for the digital implementation of baseband functionalities with a 1.32 Gsample/s chip rate analog-to-digital converter. An initial timing acquisition algorithm and a data demodulation method are also studied. The proposed searcher effectively acquires initial symbol and frame timing during the preamble transmission period. A hardware efficient receiver structure using 24 parallel digital correlators for binary phase-shift keying DS-UWB transmission is presented. The proposed correlator structure operating at 55 MHz is shared for correlation operations in a searcher, a channel estimator, and the demodulator of a RAKE receiver. We also present a pseudo-random noise sequence generated with a primitive polynomial, $1+x^2+x^5$, for packet detection, automatic gain control, and initial timing acquisition. Simulation results show that the performance of the proposed parallel processing searcher employing the presented pseudo-random noise sequence outperforms that employing a preamble sequence in the IEEE 802.15.3a DS-UWB proposal.

Keywords: Direct sequence ultra-wideband (DS-UWB), timing acquisition, searcher, correlator, parallel processing.

I. Introduction

In designing a direct sequence ultra-wideband (DS-UWB) system, three kinds of structures are considered according to the sampling rate of an analog-to-digital (A/D) converter at the receiver. The first structure employs a symbol rate A/D converter, which utilizes an analog correlator [1]. The second structure adopts a chip rate A/D converter. The received radio frequency (RF) signals from the air are converted to baseband signals by the RF receiver and are then passed through the chip rate A/D converter, which is followed by the baseband modem [2], [3]. Accordingly, we should employ a digital correlator. The third structure uses a Nyquist rate A/D converter operating at tens of GHz, which processes the received signals directly at the passband [4]. In this paper, we present a baseband modem receiver employing a chip rate A/D converter operating over one GHz. The DS-UWB system proposed in the paper is based on binary phase-shift keying (BPSK) modulation occupying the spectrum from 3.1 GHz to 4.85 GHz, which is adopted as mandatory mode in the DS-UWB proposal [5].

Recently, many studies have discussed DS-UWB systems, whereas there have been almost no studies dealing with the digital correlator structure for BPSK modulated signal in the DS-UWB receiver [6]-[8]. We propose a structure with 24 parallel digital correlators operating at a 55 MHz symbol clock so as to implement a high-speed baseband receiver. Although there are various methods for acquiring initial synchronization [9]-[11], it is not easy to efficiently apply the existing methods to the DS-UWB system, which requires an ultra-wide bandwidth and fast operating speed. We present a parallel processing searcher structure, operating at 55 MHz, which can jointly acquire initial symbol and frame synchronization during the preamble transmission period.

Manuscript received Dec. 4, 2007; revised June 20, 2008; accepted June 27, 2008.

This work was supported by the IT R&D program of MKE/IITA [2006-S-071-02, Development of UWB Solution for High Speed Multimedia Transmission].

Kyu-Min Kang (phone: + 82 42 860 6703, email: kmkang@etri.re.kr) and Sang-Sung Choi (email: sschoi@etri.re.kr) are with the IT Convergence Technology Research Laboratory, ETRI, Daejeon, Rep. of Korea.

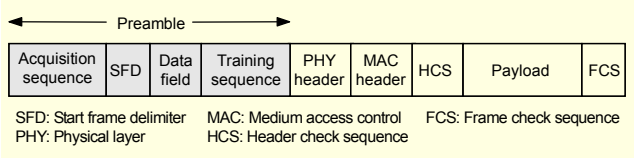

Fig. 1. PHY frame format in a DS-UWB system.

The remainder of this paper is organized as follows. The next section briefly discusses transmit signal and channel models for the DS-UWB data transmission. In section III, we present a hardware efficient digital correlator structure with shared logics. We also propose a parallel processing searcher for initial symbol and frame timing acquisition in section IV. Simulation results are given in section V, and a summary and conclusions are presented in section VI.

II. DS-UWB Data Transmission

1. Physical Layer Frame Format

Figure 1 shows a physical layer (PHY) frame format applied to the DS-UWB system [5]. The DS-UWB preamble contains an acquisition sequence, a start frame delimiter marker, a training data field, and a variable-length pseudo-random noise (PN) equalizer training sequence. An acquisition sequence, a training sequence, and a header check sequence are generated from a baseband modem. A PHY header and a medium access control (MAC) header are generated from a MAC and transmitted to the baseband modem. During the payload transmission period, a baseband receiver module, including a RAKE receiver, a tracker, an equalizer, and a Viterbi decoder, is continuously operated to recover the received data by using the information obtained during the preamble transmission period (See [5] for more details).

2. Spreading Code

Tables 1, 2, and 3 show spreading codes for the code lengths M=24, 12, 6, 4, 3, 2, and 1 that are applicable to BPSK transmission in the DS-UWB system. Note that there are 6 code sets for 6 piconet channels in the lower band occupying the spectrum from 3.1 GHz to 4.85 GHz. For each piconet channel, there is a designated chip rate and a center frequency [5]. Various data rates from 27.5 Mbps to 1.32 Gbps are supported by employing various lengths of spreading codes given in Tables 1, 2, and 3.

3. Acquisition Sequence

The preamble starts with the acquisition sequence, which is used for initial synchronization, automatic gain control (AGC), automatic frequency control (AFC), and channel estimation. In [1], the DS-UWB group proposed an 825-symbol preamble sequence for the low-band medium-length sequence. Later, a PN acquisition sequence generated from a length 17 linear feedback shift register (LFSR) with rotating seed was proposed in [3] and [5] because the autocorrelation characteristic of the 825-symbol preamble sequence is not good enough. Similarly, we propose two kinds of acquisition sequences in the paper. The first is a PN sequence generated with the primitive polynomial $1+x^2+x^5$, which is used for packet detection, AGC, and initial timing acquisition. We employ 16 repetitions of the 32-symbol sequence. The second PN sequence is generated from a length 17 LFSR with the primitive polynomial $1+x^{14}+x^{17}$, which is used for synchronization verification, channel estimation, and AFC. In section V, we specifically compare the characteristics of the 825-symbol preamble sequence and the proposed PN sequence generated with the primitive polynomial $1+x^2+x^5$.

Table 1. Ternary spreading code of length 24 for BPSK transmission.

Code set number	M=24 codes
1	-1, 0, 1, -1, -1, -1, 1, 1, 0, 1, 1, 1, 1, -1, 1, -1, 1, 1, 1, -1, 1, -1, -1, 1
2	-1, -1, -1, -1, 1, -1, 1, -1, 1, -1, -1, 1, -1, 1, 1, -1, -1, 1, 1, 0, -1, 0, 1, 1
3	-1, 1, -1, -1, 1, -1, -1, 1, -1, 0, -1, 0, -1, -1, 1, 1, 1, -1, 1, 1, 1, -1, -1, -1
4	0, -1, -1, -1, -1, -1, -1, 1, 1, 0, -1, 1, 1, -1, 1, -1, -1, 1, 1, 1, -1, 1, -1, 1, -1
5	-1, 1, -1, 1, 1, -1, 1, 0, 1, 1, 1, -1, -1, 1, 1, -1, 1, 1, 1, -1, -1, -1, 0, -1
6	0, -1, -1, 0, 1, -1, -1, 1, -1, -1, 1, 1, 1, 1, -1, -1, 1, -1, 1, -1, 1, 1, 1, 1

Table 2. Ternary spreading code of length 12 for BPSK transmission.

Code set number	M=12 codes
1	0, -1, -1, -1, 1, 1, 1, -1, 1, 1, -1, 1
2	-1, 1, -1, -1, 1, -1, -1, -1, 1, 1, 1, 0
3	0, -1, 1, -1, -1, 1, -1, -1, -1, 1, 1, 1
4	-1, -1, -1, 1, 1, 1,-1, 1, 1, -1, 1, 0
5	-1, -1, -1, 1, 1, 1, -1, 1, 1, -1, 1, 0
6	0, -1, -1, -1, 1, 1, 1,-1, 1, 1, -1, 1

Table 3. Length 6 and shorter spreading codes for BPSK transmission.

Code set numbers	M=6	M=4	M=3	M=2	M=1
1 through 6	1, 0, 0, 0, 0, 0	1, 0, 0, 0	1, 0, 0	1, 0	1

4. Transmit Signal Model

A DS-UWB transmitter employs a spreading code having a

length of M for BPSK transmission. The data symbol is spread by the spreading code and then fed to a pulse shaping filter. The passband transmit signal is expressed as

$$s(t) = \sum_{n=-\infty}^{\infty} \left\{ a_n \sum_{m=0}^{M-1} c_m g(t - nT - mT_c) \right\} \cdot \sqrt{2} \cos 2\pi f_c t \ , \tag{1}$$

where $a_n, a_n \in \{1, -1\}$, denotes the data symbol for the period nT, and T is the symbol interval. The sequence $\{c_m\}$ denotes the spreading code; T_c is the chip interval and is equal to T/M; $g(t)$ is the transmit pulse shaping filter [5], [12], [13]; and f_c denotes carrier frequency.

5. UWB Channel Model

We briefly discuss a UWB channel model proposed by Foerster in [14]. To evaluate the PHY performance of UWB systems, the channel model is derived from the Saleh-Valenzuela model [15] with a log-normal fading distribution rather than a Rayleigh distribution for the multi-path gain magnitude, which is based on a number of measurements. Independent fading is assumed for each cluster as well as each ray within the cluster. The channel impulse response can be expressed as

$$h(t) = X \sum_{l_1=0}^{L_1} \sum_{l_2=0}^{L_2} \alpha_{l_2,l_1} \delta(t - T_{l_1} - \tau_{l_2,l_1}) , \tag{2}$$

where X represents the log-normal shadowing, α_{l_2,l_1} is the multi-path gain coefficient, T_{l_1} is the arrival time of the first path of the l_1th cluster, and τ_{l_2,l_1} is the delay of the l_2th path within the l_1th cluster relative to the first path arrival time. The cluster arrival time and subsequent rays are modeled as Poisson arrival processes. Note that four channel models, CM1 to CM4, are reported in [14].

6. Receiver Front-End

The baseband equivalent of the received signal is given by

$$\begin{aligned} r(t) &= r_I(t) + j r_Q(t) \\ &= LPF\left\{ \left(s(t) * h(t) + \tilde{n}(t) \right) \cdot \sqrt{2} e^{j2\pi(f_c + \Delta f)t} \right\}, \end{aligned} \tag{3}$$

where $LPF(\cdot)$ stands for low-pass filtering, * denotes convolution operation, $\tilde{n}(t)$ is zero-mean additive white Gaussian noise (AWGN) with two-sided power spectral density $N_0/2$, and Δf is assumed to be the frequency offset in hertz. The passband transmit signal is transmitted through the UWB channel with impulse response $h(t)$. The signal component can be rewritten as

$$\begin{aligned} s(t) * h(t) &= \int_{-\infty}^{\infty} s(t-\tau) h(\tau) d\tau \\ &= X \sum_{l_1=0}^{L_1} \sum_{l_2=0}^{L_2} \alpha_{l_2,l_1} \sum_{n=-\infty}^{\infty} \left\{ a_n \sum_{m=0}^{M-1} c_m g(t - T_{l_1} - \tau_{l_2,l_1} - nT - mT_c) \right\} \\ &\quad \cdot \sqrt{2} \cos 2\pi f_c (t - T_{l_1} - \tau_{l_2,l_1}). \end{aligned} \tag{4}$$

After some straightforward calculation, we have the inphase and quadrature baseband received signals as

$$\begin{aligned} r_I(t) &= X \sum_{l_1=0}^{L_1} \sum_{l_2=0}^{L_2} \alpha_{l_2,l_1} \sum_{n=-\infty}^{\infty} \left\{ a_n \sum_{m=0}^{M-1} c_m g(t - T_{l_1} - \tau_{l_2,l_1} - nT - mT_c) \right\} \\ &\quad \cdot \cos 2\pi \left(f_c (T_{l_1} + \tau_{l_2,l_1}) + \Delta f t \right) \\ &\quad + n_I(t) \ , \end{aligned} \tag{5a}$$

$$\begin{aligned} r_Q(t) &= X \sum_{l_1=0}^{L_1} \sum_{l_2=0}^{L_2} \alpha_{l_2,l_1} \sum_{n=-\infty}^{\infty} \left\{ a_n \sum_{m=0}^{M-1} c_m g(t - T_{l_1} - \tau_{l_2,l_1} - nT - mT_c) \right\} \\ &\quad \cdot \sin 2\pi \left(f_c (T_{l_1} + \tau_{l_2,l_1}) + \Delta f t \right) \\ &\quad + n_Q(t) \ , \end{aligned} \tag{5b}$$

where the inphase and quadrature baseband white Gaussian noise $n_I(t)$ and $n_Q(t)$ are expressed as

$$n(t) = n_I(t) + j n_Q(t) = LPF\left(\tilde{n}(t) \cdot \sqrt{2} e^{j2\pi(f_c + \Delta f)t} \right). \tag{6}$$

III. Digital Correlator and Its Operation

In the DS-UWB receiver, a hardware efficient digital correlator structure with shared logics is necessary because many correlation operations are required for initial timing acquisition, channel estimation, and the data demodulation of a RAKE receiver. In this section, we present a structure with 24 parallel digital correlators which is simultaneously applicable to all kinds of spreading codes and receiver modules used for correlation operations.

1. Parallel Digital Correlators

Figure 2 shows 24 parallel digital correlators and receiver modules used for the correlation operation in the DS-UWB system. The A/D converter digitizes the analog input signal at a 1.32 GHz sampling rate. The received discrete-time complex input signals $r(n,k)$, $k = 0,1,\cdots,23$, are then stored in an upper 24-chip buffer, where n and k denote time indices with the symbol and chip duration, respectively. Note that the

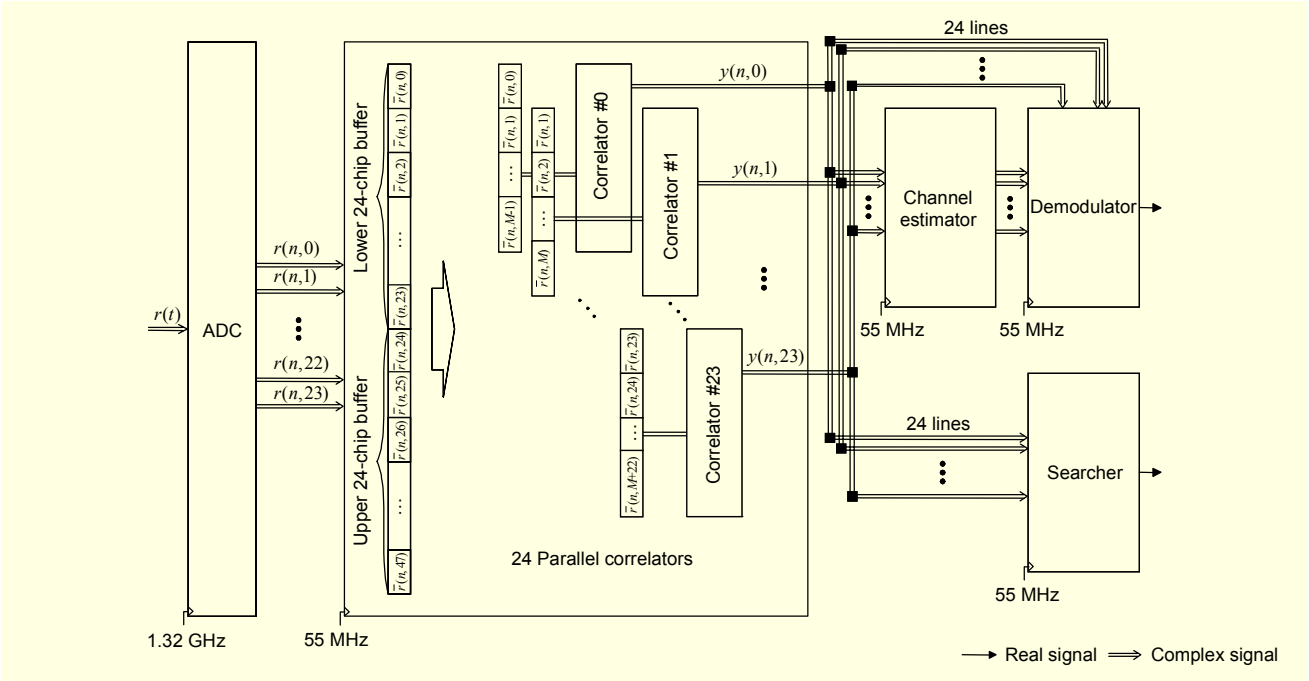

Fig. 2. Hardware efficient parallel digital correlators and receiver modules used for the correlation operation in the DS-UWB system.

previously stored 24-chip input signals in the upper buffer move to a lower 24-chip buffer as follows:

$$\begin{aligned} &\overline{r}(n,k) = \overline{r}(n-1,24+k), \\ &\overline{r}(n,24+k) = r(n,k), \qquad k = 0,1,\cdots,23. \end{aligned} \tag{7}$$

From the data stored in the 48-chip buffer, we construct 24 parallel buffers, each with the length of M. Thus, we obtain the input values for the 24 parallel correlators. The parallel correlator structure operates on a 55 MHz clock, which corresponds to the symbol rate of the DS-UWB system employing the spreading code of length $M = 24$. To simplify the analysis, we assume the transmit pulse shaping filter $g(t)$ to be a unit amplitude rectangular pulse of duration T_c. We also assume that the frequency offset is perfectly compensated. The complex input signal $\overline{r}(n,k)$ can then be rewritten as

$$\begin{aligned} \overline{r}(n,k) &= \overline{r}_I(n,k) + j\overline{r}_Q(n,k) \\ &= X\sum_{l_1=0}^{L_1}\sum_{l_2=0}^{L_2} \alpha_{l_2,l_1}\hat{a}_{n-Q_M(k)}c_{R_M(k)}e^{j2\pi f_c(T_{l_1}+\tau_{l_2,l_1})} + n(k), \end{aligned} \tag{8}$$

where $\overline{r}_I(n,k)$ and $\overline{r}_Q(n,k)$ represent the inphase and quadrature components of $\overline{r}(n,k)$, respectively. Here, $\hat{a}_n = a_{n-D}$ is the desired symbol after the overall processing delay of D symbol time intervals. The notations $Q_M(k)$ and $R_M(k)$ are defined as the quotient and remainder of $(k - T_{l_1} - \tau_{l_2,l_1})$ when divided by M, respectively, where $R_M(k)$ corresponds to one of the integer values from 0 to M–1.

The correlation value $y(n,k)$ is given by

$$\begin{aligned} y(n,k) &= y_I(n,k) + jy_Q(n,k) \\ &= \sum_{i=0}^{M-1} \overline{r}(n,i+k)c_i, \quad k = 0,1,\cdots,23, \end{aligned} \tag{9}$$

where $y_I(n,k)$ and $y_Q(n,k)$ represent the inphase and quadrature components of $y(n,k)$, respectively. A correlator for the correlation operation of the received complex input signal and the known ternary spreading code of length M is shown in Fig. 3. Here, the real and imaginary part correlation operators have the same structure and correlate the respective input values with an M-length spreading code to thereby obtain respective resultant values. The correlation value $y(n,k)$ can be rewritten as the sum of the main-path signal, the other multi-path signals, and noise components by using (8) and (9):

$$\begin{aligned} y(n,k) &= X\sum_{i=0}^{M-1} \alpha_{p_2,p_1}\hat{a}_{n-Q_M(i+k)}c_{R_M(i+k)}c_i e^{j2\pi f_c(T_{p_1}+\tau_{p_2,p_1})} \\ &\quad + X\sum_{i=0}^{M-1}\sum_{(l_1,l_2)=(0,0)}^{(L_1,L_2)} \alpha_{l_2,l_1}\hat{a}_{n-Q_M(i+k)}c_{R_M(i+k)}c_i e^{j2\pi f_c(T_{l_1}+\tau_{l_2,l_1})} \\ &\quad + \sum_{i=0}^{M-1} n(i+k)c_i \ , \end{aligned} \tag{10}$$

where $l_1 = 0,1,\cdots,L_1$, $l_2 = 0,1,\cdots,L_2$, and $(l_1,l_2) \neq (p_1,p_2)$. Here, $(T_{p_1} + \tau_{p_2,p_1})$ is assumed to be the time delay of the

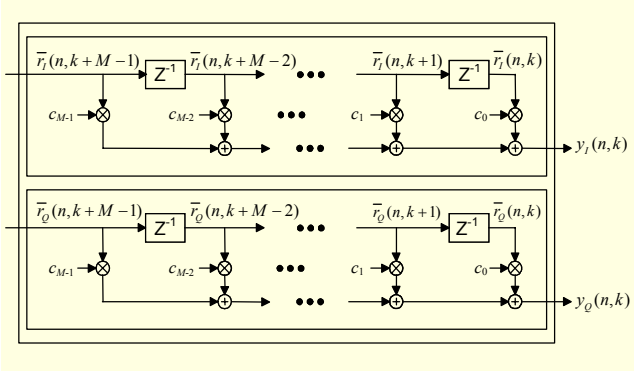

Fig. 3. Correlator structure for complex input.

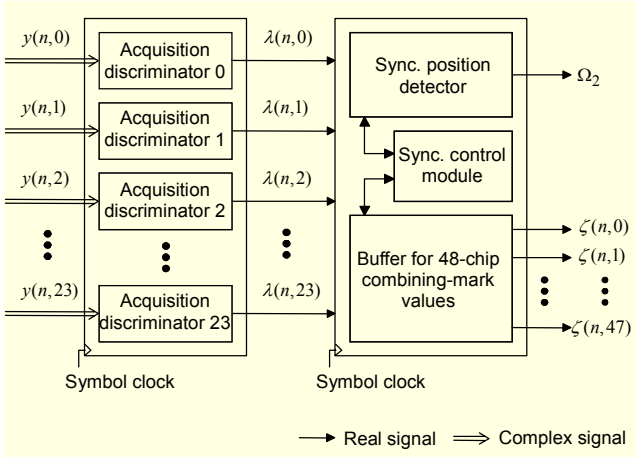

Fig. 4. Parallel processing searcher structure for acquiring an initial synchronization of a DS-UWB modem.

main-path, and therefore, the correlation value is maximum when k equals $(T_{p_1}+\tau_{p_2,p_1})$.

2. Correlation Operation for Timing Acquisition, Channel Estimation, and Demodulation

In the DS-UWB receiver, if the correlators are separately implemented for the correlation operation of different code lengths, the complexity of the receiver may significantly increase. As discussed in the previous subsection, we just employ a structure using 24 parallel digital correlators at the receiver. In the initial timing acquisition and channel estimation modes, the DS-UWB system uses the ternary spreading code of length 24. Thus, the 24 parallel correlation result values correspond to one symbol interval. Meanwhile, in the payload transmission mode, data is transferred with various kinds of spreading codes as shown in Tables 1, 2, and 3. For code length 24, the 24 correlation result values correspond to one symbol interval, and for code length 12, the resultant values correspond to 2 symbol intervals. However, when data is transferred by using a spreading code with a length of 6 or less, the receiver modules directly use the output values of the A/D converter instead of the resultant values of the correlator. In such cases, the 24 correlation result values for the spreading code lengths M=6, 4, 3, 2, and 1 correspond to 4, 6, 8, 12, and 24 symbol intervals, respectively. In this manner, the parallel digital correlator structure, employing just one clock scheme, operating at 55 MHz, enables the DS-UWB receiver to support available data rates from tens of Mbps up to 1.32 Gbps.

IV. Initial Symbol and Frame Timing Acquisition

We discuss a DS-UWB receiver using spreading codes of the length $M=24$ with BPSK modulation [5]. In this section, we propose a searcher structure for initial timing acquisition within a relatively short preamble transmission period. After jointly acquiring symbol and frame synchronization, a synchronization position value and 48-chip combining-mark values are stored in a register. Note that 48-chip size corresponds to two symbol intervals.

1. Parallel Processing Searcher

Figure 4 shows a parallel processing searcher structure for acquiring the initial synchronization of the DS-UWB baseband modem, which consists of 24 parallel timing acquisition discriminators, a synchronization control module, a synchronization position detector, and a 48-chip buffer for storing combining-mark values. The 24 parallel initial timing acquisition discriminators determine whether correlation values $y(n,k)$, passed from the 24 parallel correlators, exceed threshold values, and then output 24 resultant values $\lambda(n,k)$. The synchronization position detector is a module for detecting a timing acquisition position value, Ω_2. The 48-chip buffer is used to store combining-mark values, $\zeta[n,j]$ for j=0, 1,⋯, 47. The synchronization control module stores the 24 resultant values passed from the synchronization discriminator module in the 48-chip buffer and controls the schedule of the synchronization position detector so as to achieve the acquisition position value, Ω_2, by using the 48-chip combining-mark values. Note that the obtained synchronization position value and the 48-chip combining-mark values are used for data demodulation. All the modules in the searcher are operated with a 55 MHz symbol clock.

2. Initial Timing Acquisition Discriminator

Figure 5 shows a detailed block diagram of the k-th initial timing acquisition discriminator of the 24 parallel timing acquisition discriminators used in the searcher shown in Fig. 4. Each timing acquisition discriminator is designed to perform N_1 symbol coherent combinations and noncoherent

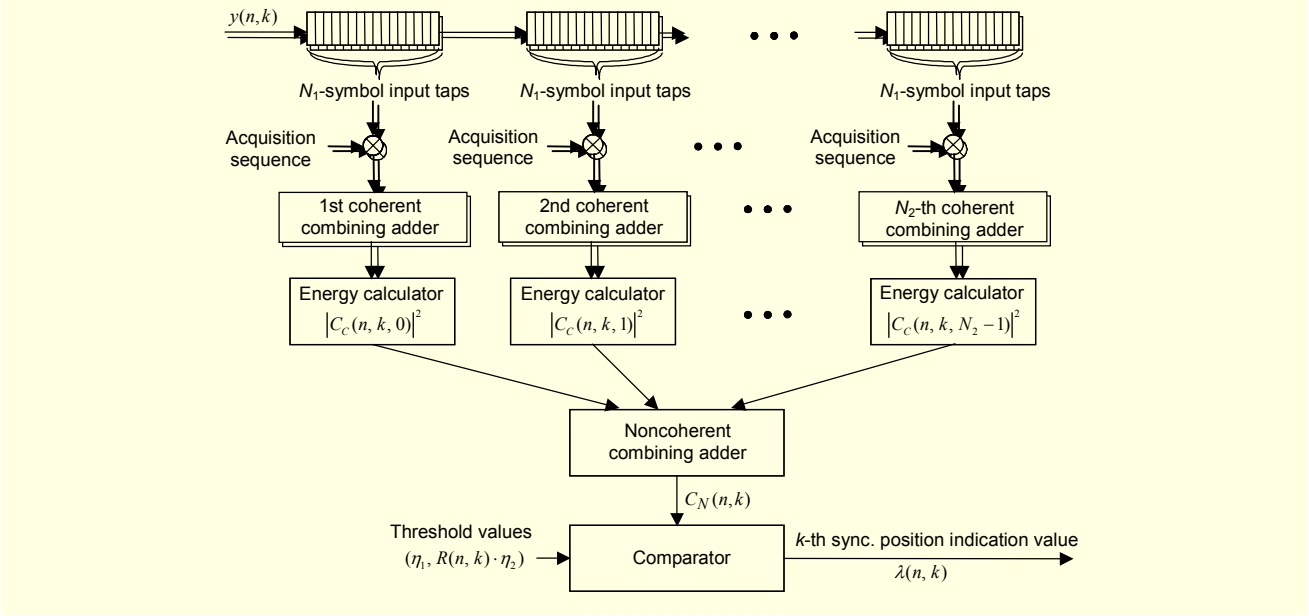

Fig. 5. Initial timing acquisition discriminator in the searcher.

combinations with N_2 energy outputs. The despread complex values, $y(n,k)$, passed from the k-th correlator, are utilized as input signals in the k-th timing acquisition discriminator, and $N_1 \times N_2$ complex input values corresponding to the despread values of $N_1 \times N_2$ symbol intervals are aggregately stored in the $N_1 \times N_2$ input filter taps of the k-th timing acquisition discriminator. Symbol matched filters conduct coherent combining operations for successive N_2 pairs of N_1 symbol taps with a predetermined preamble pattern of $N_1 \times N_2$ symbol intervals, and thereby output N_2 pairs of coherent combining resultant values. The β-th coherent combining resultant value corresponding to the k-th chip period of the n-th symbol time is given by

$$C_C(n,k,\beta) = \sum_{j=0}^{N_1-1} y(n-\beta N_1 - j, k)\tilde{p}_{\beta N_1 + j}\ , \quad \beta = 0,1,\cdots,N_2-1\ , \tag{11}$$

where $\tilde{p}_i$, $(i = 0, 1, \cdots, N_1 \times N_2 - 1)$ denotes the predetermined acquisition sequence in reverse order. N_2 energy values of energy calculators obtained by adding an inphase value and a quadrature value of each N_2 pairs of coherent combining values are fed to a noncoherent combining adder for noncoherent combining. The noncoherent combining value corresponding to the k-th chip period of the the n-th symbol time is now obtained as

$$C_N(n,k) = \sum_{\beta=0}^{N_2-1} \left| C_C(n,k,\beta) \right|^2 . \tag{12}$$

A comparator compares the noncoherent combining value with threshold values as

$$C_N(n,k) > \eta_1 \quad \text{and} \quad C_N(n,k) > R(n,k)\cdot\eta_2\ , \tag{13}$$

where the power of the length N_3 despread complex input values is given by

$$R(n,k) = \sum_{i=0}^{N_3-1} \left| y(n-i,k) \right|^2 . \tag{14}$$

If the noncoherent combining value satisfies the two conditions in (13), 1 is assigned to the k-th synchronization position indication value $\lambda(n,k)$; if not, 0 is assigned. Note that the preamble pattern of $N_1 \times N_2$ symbol intervals are utilized for the symbol matched filtering, and δ symbol intervals are additionally employed for switchover to the next preamble patterns of the symbol matched filters in consideration of the operation speed of the initial timing acquisition algorithm. Also, the symbol matched filters output corresponding results at every symbol input and are operated until the initial synchronization is acquired. In this manner, we can design the initial timing acquisition discriminator with the coherent and noncoherent combining adders, energy calculators, and comparator, which is adequate for the channel environment or receiver architecture.

3. Initial Timing Acquisition Algorithm

We briefly summarize the initial timing acquisition algorithm, where time index k=0, 1,⋯, 23.

Step 1. Assign 0 to an acquisition indicator γ_1.

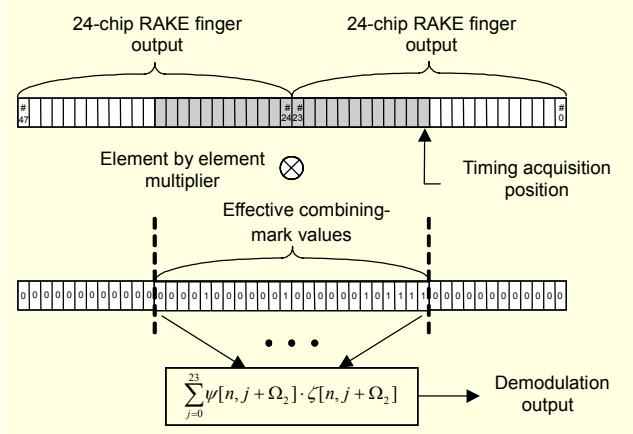

Fig. 6. Data demodulation method with a timing acquisition position value and combining-mark values.

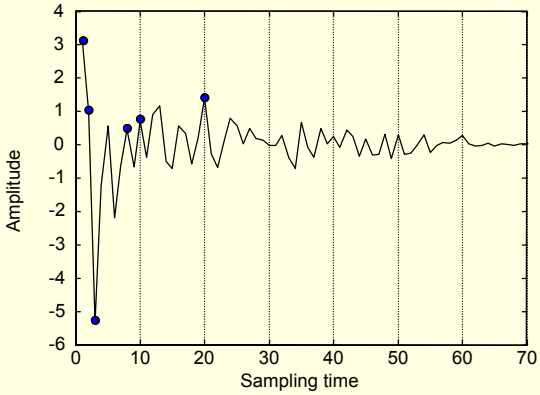

Fig. 7. Example of the discrete-time UWB channel impulse response corresponding to the 0 to 4 m LOS channel environment (CM1) with tap spacing of 1/1.32 ns.

Step 2. Move combining-mark values in the upper 24-chip buffer, $\zeta[n-1,k+24]$, to the lower 24-chip buffer, $\zeta[n,k]$.

Step 3. Store the synchronization position indication values, $\lambda(n,k)$, in the upper 24-chip buffer, $\zeta[n,k+24]$.

Step 4. Check 24 combining-mark values in the lower 24-chip buffer, $\zeta[n,k]$, from k=0 to 23.

Step 5. If $\zeta[n,k]=0$ for every k, repeat the first timing acquisition mode from steps 1 to 4.

Step 6. If $\zeta[n,k]=1$ for an arbitrary k, assign k to a timing acquisition position value Ω_1, which corresponds to the time index for the first occurrence of $\zeta[n,k]=1$. Note that multiple combining-mark values may become 1s in the multi-path channel environment. Thereafter, assign 1 to the acquisition indicator γ_1, and go to verification mode (step 7).

Step 7. In the verification mode (γ_1=1), repeat the previous steps until $\zeta[n,k]$ is equal to 1 with a predetermined preamble pattern of $N_1 \times N_2$ symbol intervals during the next $N_1 \times N_2 + \delta$ symbol periods, and find the second timing acquisition position value Ω_2. Then, compare the acquisition position value Ω_2 obtained in the verification mode and the stored acquisition position value Ω_1 obtained in first timing acquisition mode. If $\Omega_2 = \Omega_1$, the searcher achieves the final timing acquisition position value and 48-chip combining-mark values. Otherwise, if $\Omega_2 \neq \Omega_1$, assign 0 to the acquisition indicator γ_1, and go to the first timing acquisition mode.

4. Data Demodulation

Figure 6 illustrates a method applied to the data demodulation operation with the timing acquisition position value and 48-chip combining-mark values. The timing acquisition position value and combining-mark values stored in the register during the initial timing acquisition period are utilized in estimating a channel variation through a tracking process (which is not discussed in the paper) performed during the data transmission period. The timing acquisition position value and combining-mark values are also continuously updated for the demodulation operation. As shown in Fig. 6, data demodulation is performed with reference to 24 successive combining-mark values starting from the timing acquisition position, out of the 48 combining-mark values. Suppose that the output of the RAKE fingers in the 48-chip buffer at the n-th symbol time is $\psi[n,j]$ for j=0, 1,⋯, 47. The demodulation output at the n-th symbol time is then given by

$$\Psi(n) = \sum_{j=0}^{23} \psi[n, j+\Omega_2] \cdot \zeta[n, j+\Omega_2]. \qquad (15)$$

That is, if a referred combining-mark value is 1, the resultant value of the corresponding RAKE receiver finger is utilized in performing the demodulation process; otherwise, if a referred combining-mark value is 0, the resultant value is not utilized.

V. Simulation Results and Discussion

Figure 7 shows an example of the discrete-time UWB channel impulse response corresponding to the 0 to 4 m line-of-sight (LOS) channel environment (CM1) with tap spacing of 1/1.32 ns [14]. As shown in the figure, a large number of RAKE fingers are required to sufficiently capture multi-path energy. That is, we should employ more than 20 RAKE fingers with a time span of 1/1.32 ns. An equalizer should also be adopted to mitigate the effect of intersymbol interference. Note that the channel impulse response of Fig. 7 is utilized in the simulations of Figs. 8, 10, and 11. Figures 8(a) and (b) show correlation values obtained by employing the 825-symbol preamble sequence presented in [1], and the proposed PN

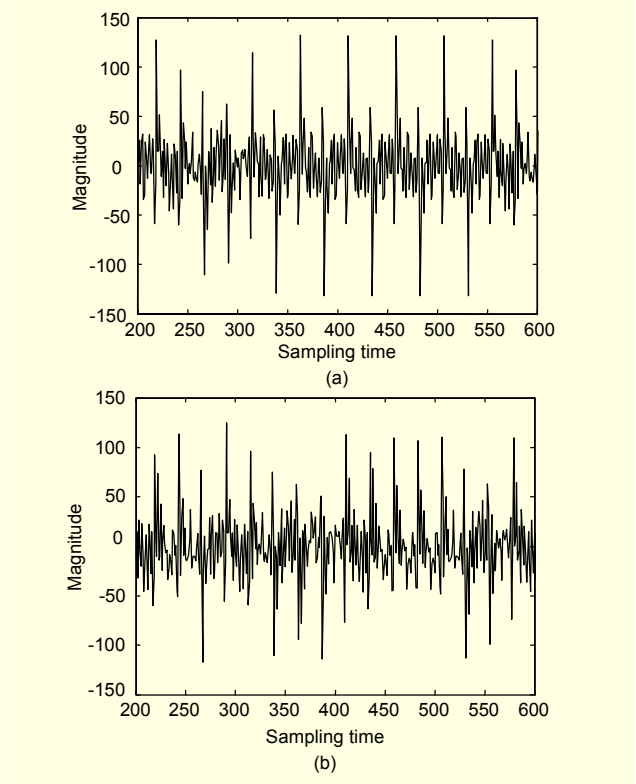

Fig. 8. (a) Correlation values obtained by employing the preamble pattern suggested in the IEEE 802.15.3a DS-UWB proposal and (b) correlation values obtained by employing the proposed PN sequence.

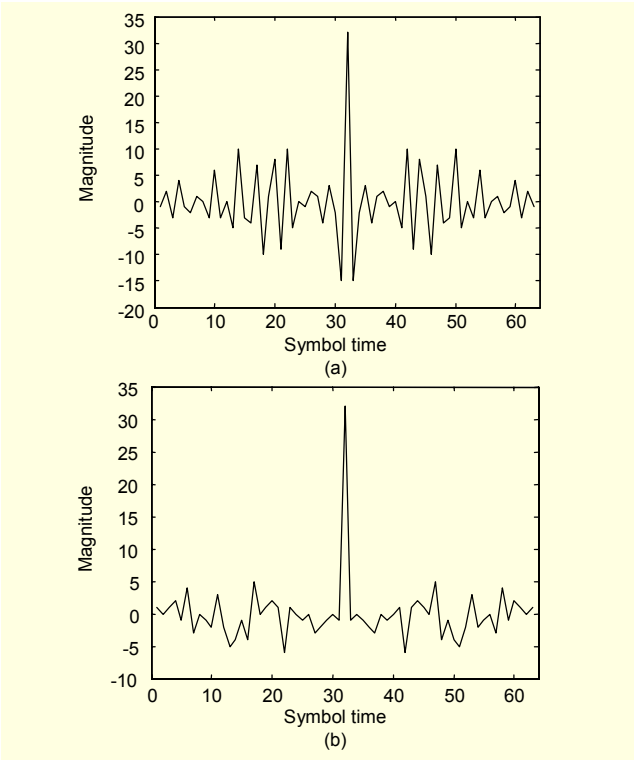

Fig. 9. (a) Autocorrelation of a 32-symbol preamble pattern from the 825-symbol preamble sequence in the IEEE 802.15.3a DS-UWB proposal and (b) autocorrelation of the PN sequence generated with primitive polynomial $1+x^2+x^5$.

sequence with the primitive polynomial $1+x^2+x^5$, respectively, where the spreading code of length 24 is used. The mainlobe-to-peak sidelobe ratios [16] for the correlation of the received signal and the length-24 ternary spreading code in the UWB channel environment are similar for both cases. However, the autocorrelation characteristic of the 825-symbol preamble sequence is not good enough for initial timing acquisition. Figure 9 compares the autocorrelation of a 32-symbol preamble pattern from the 825-symbol preamble sequence in the IEEE 802.15.3a DS-UWB proposal, and the auto-correlation of the 32-symbol PN sequence generated with the primitive polynomial $1+x^2+x^5$. As shown in Figs. 9(a) and (b), the proposed PN sequence is more appropriate for the preamble pattern of symbol-matched filters than the 825-symbol preamble sequence in the IEEE 802.15.3a DS-UWB proposal.

Figure 10 shows coherent combining outputs of the k-th initial timing acquisition discriminator corresponding to k=1, 2, 3, 8, 10, and 20, which use a 32-symbol preamble pattern from the 825-symbol preamble sequence in the IEEE 802.15.3a DS-UWB proposal. Coherent combining outputs obtained by employing the 32-symbol PN sequence generated with the primitive polynomial $1+x^2+x^5$ are also given in Fig. 11. To ascertain the characteristics of the timing acquisition

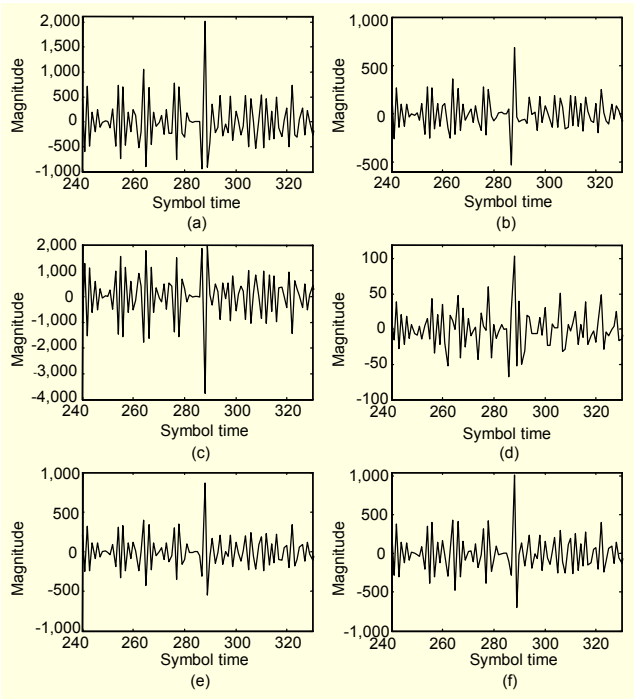

Fig. 10. Coherent combining output of the k-th acquisition discriminator, which uses a 32-symbol preamble pattern from the 825-symbol preamble sequence in the IEEE 802.15.3a DS-UWB proposal. (a) k=1, (b) k=2, (c) k=3, (d) k=8, (e) k=10, and (f) k=20.

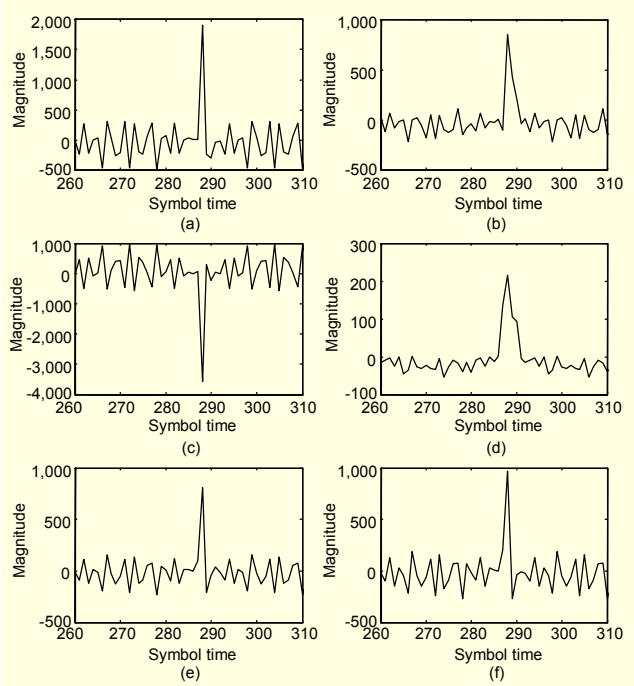

Fig. 11. Coherent combining output of the k-th acquisition discriminator, which uses the 32-symbol PN sequence generated with the primitive polynomial $1+x^2+x^5$. (a) k=1, (b) k=2, (c) k=3, (d) k=8, (e) k=10, and (f) k=20.

discriminators depending on preamble sequence, timing offset and frequency offset are assumed to be 0. In Figs. 10 (a) to (f), the peak absolute magnitude of the third acquisition discriminator output is the largest, whose position corresponds to the main-path of Fig. 7. Figure 10 also shows that the acquisition discriminator outputs have relatively large magnitude around the peak values because the autocorrelation characteristic of the preamble pattern is poor as in Fig. 9(a). Therefore, we cannot effectively perform the initial timing acquisition with the 32-symbol preamble pattern from the 825-symbol preamble sequence because it is difficult to determine the threshold values properly in the low signal-to-noise ratio (SNR) UWB channel environments. As seen in Figs. 11 (a) to (f), the acquisition discriminator outputs obtained with the primitive polynomial $1+x^2+x^5$ have large magnitude at the symbol synchronization position and have small magnitude at the other positions.

In Figs. 12 and 13, we investigate the performance of the parallel processing searcher by computer simulation in the UWB channel environment, where frequency offset is assumed to be 10 ppm. The probabilities of timing acquisition have been obtained by averaging over 500 independent runs per E_b / N_0 for each channel realization (100 channel realizations in each channel model from CM1 to CM4).

Figure 12 compares the performance of the parallel processing

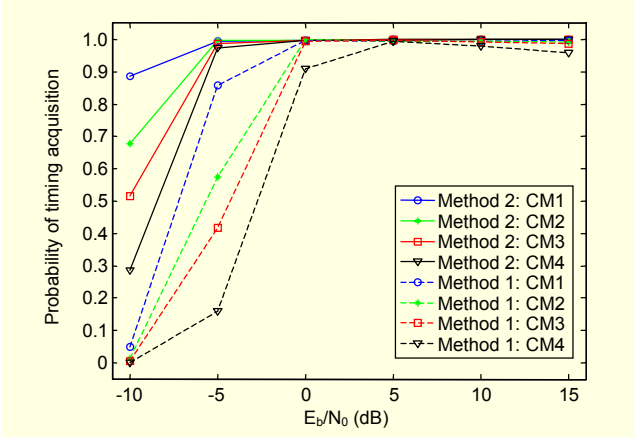

Fig. 12. Performance comparison of the parallel processing searcher with N_1=32 and N_2=1 employing a 32-symbol preamble pattern from the 825-symbol preamble sequence in the IEEE 802.15.3a DS-UWB proposal (method 1) and that employing the 32-symbol PN sequence generated with the primitive polynomial $1+x^2+x^5$ (method 2) in the CM1, CM2, CM3, and CM4 channel environments.

searcher with N_1=32 and N_2=1 employing a 32-symbol preamble pattern from the 825-symbol preamble sequence in the IEEE 802.15.3a DS-UWB proposal (method 1) and that employing the 32-symbol PN sequence generated with the primitive polynomial $1+x^2+x^5$ (method 2), which was tested on the IEEE 802.15.3a channel models CM1 to CM4 [14] in the presence of AWGN. Note that threshold values $\eta_1=5\times10^5$, η_2=11, and N_3=32 were employed. Figure 12 indicates that the timing acquisition performance of method 2 is much better than that of method 1. As discussed in Figs. 9(a) and 10, because the autocorrelation characteristic of the 32-symbol preamble pattern of the method 1 is poor, the acquisition discriminator outputs have relatively large magnitude around the peak values. Unfortunately, the timing synchronization of method 1 occasionally occurs at a wrong timing position in the relatively high SNR UWB channel, which decreases the timing acquisition probability of method 1 even when the E_b / N_0 is 10 and 15 dB, as shown in Fig. 12. From the results of Figs. 10 to 12, we can conclude that the PN sequence generated with the primitive polynomial $1+x^2+x^5$ has a good autocorrelation characteristic and, therefore, is adequate for the initial timing acquisition. Note that the probability of acquisition failure becomes less than 10^{-4} when method 2 is used with properly selected threshold values even in the CM4 channel environments having an E_b / N_0 of 0 dB.

Figure 13 compares the performance of the parallel processing searcher with different numbers of coherent and noncoherent combining operations (N_1=32, N_2=1/N_1=16, N_2=2/N_1=8, N_2=4), which employ the 32-symbol PN sequence generated with the primitive polynomial $1+x^2+x^5$ in the CM1 and CM3 channel environments. Because the parallel processing

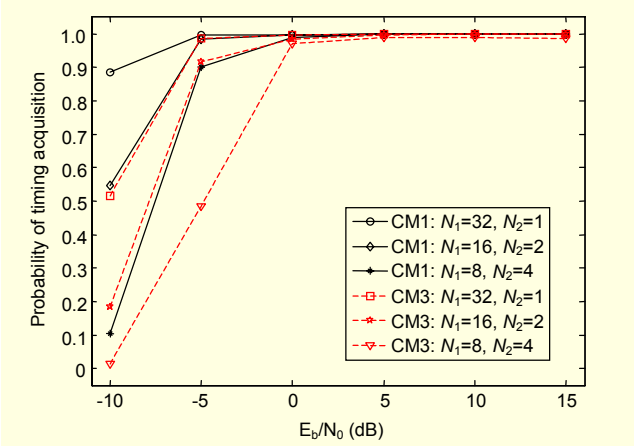

Fig. 13. Performance comparison of the parallel processing searcher with various numbers of coherent and noncoherent combining operations, where the 32-symbol PN sequence generated with the primitive polynomial $1+x^2+x^5$ in the CM1 and CM3 channel environments is employed.

searcher structure with the N_1=32 coherent combining and N_2=1 noncoherent combining can achieve the largest noncoherent combining value among the three structures, the searcher structure with N_1=32 and N_2=1 shows the best performance.

VI. Conclusion

We have discussed a DS-UWB baseband modem receiver employing a chip rate A/D converter operating at 1.32 GHz. A hardware efficient structure with 24 parallel digital correlators which is simultaneously applicable to both ternary spreading codes of lengths 24 and 12 and receiver modules used for correlation operations has been proposed. We have also proposed a parallel processing searcher structure which jointly acquires an initial symbol and frame synchronization for the high-speed and parallel processed UWB system. Therefore, it significantly reduces system complexity when compared to wireless transmission systems which employ separate modules for symbol acquisition and frame acquisition. We have suggested a PN sequence generated with the primitive polynomial $1+x^2+x^5$ for packet detection, AGC, and initial timing acquisition. Simulation and analytical results showed that the performance of the parallel processing searcher employing the proposed PN sequence outperforms that employing a 32-symbol preamble pattern from the 825-symbol preamble sequence in the IEEE 802.15.3a DS-UWB proposal in UWB channel environments.

References

[1] M. Welborn and M.M. Laughlin, "Merger #2 Proposal DS-CDMA," *IEEE P802.15-03/334r2*, Sept. 2003.

[2] B.H. Park et al., "A 3.1 to 5 GHz CMOS Transceiver for DS-UWB Systems," *ETRI Journal,* vol. 29, no. 4, Aug. 2007, pp. 421-429.

[3] M. Welborn, "DS-UWB Responses to TG3a Voter no Comments," *IEEE P802.15-05/0050r2*, Jan. 2005.

[4] G.H. Im and K.M. Kang, "Performance of a Hybrid Decision Feedback Equalizer Structure for CAP-Based DSL Systems," *IEEE Trans. Signal Processing,* vol. 49, no. 8, Aug. 2001, pp. 1768-1785.

[5] R. Fisher et al., "DS-UWB Physical Layer Submission to 802.15 Task Group 3a," *IEEE P802.15-04/0137r4*, Jan. 2005.

[6] H. Sato and T. Ohtsuki, "Frequency Domain Channel Estimation and Equalisation for Direct Sequence Ultra-wideband (DS-UWB) System," *IEE Proc. Comm.*, vol. 153, no. 1, Feb. 2006, pp. 93-98.

[7] S.R. Aedudodla, S. Vijayakumaran, and T.F. Wong, "Acquisition of Direct-Sequence Transmitted Reference Ultra-wideband Signals," *IEEE J. Sel. Areas Comm.*, vol. 24, no. 4, Apr. 2006, pp. 759-765.

[8] A.M. Tonello and R. Rinaldo, "A Time-Frequency Domain Approach to Synchronization, Channel Estimation, and Detection for DS-CDMA Impulse-Radio Systems," *IEEE Trans. Wireless Comm.*, vol. 4, no. 6, Nov. 2005, pp. 3005-3017.

[9] R.R. Rick and L.B. Milstein, "Optimal Decision Strategies for Acquisition of Spread-Spectrum Signals in Frequency-Selective Fading Channels," *IEEE Trans. Comm.*, vol. 46, no. 5, May 1998, pp. 686-694.

[10] E. Sourour and S.C. Gupta, "Direct-Sequence Spread-Spectrum Parallel Acquisition in Nonselective and Frequency-Selective Rician Fading Channels," *IEEE J. Sel. Areas Comm.*, vol. 10, no. 3, Apr. 1992, pp. 535-544.

[11] Y. Wang and K.H. Chang, "Double-Dwell Hybrid Acquisition in a DS-UWB System," *ETRI Journal,* vol. 29, no. 1, Feb. 2007, pp. 1-7.

[12] S.S. Tan, A. Nallanathan, and B. Kannan, "Performance of DS-UWB Multiple-Access Systems with Diversity Reception in Dense Multipath Environments," *IEEE Trans. Veh. Technol.*, vol. 55, no. 4, July 2006, pp. 1269-1280.

[13] K.M. Kang et al., "FIR Filter of DS-CDMA UWB Modem Transmitter," *IEICE Trans. Comm.*, vol. E91-B, no. 3, Mar. 2008, pp. 907-909.

[14] J. Foerster, "Channel Modeling Sub-Committee Report Final," *IEEE P802.15-02/368r5-SG3a*, Dec. 2002.

[15] A. Saleh and R. Valenzuela, "A Statical Model for Indoor Multipath Propagation," *IEEE J. Sel. Areas Comm.*, vol. 5, no. 2, Feb. 1987, pp. 128-137.

[16] K.J. Gartz, "Generation of Uniform Amplitude Complex Code Sets with Low Correlation Sidelobes," *IEEE Trans. Signal Process.*, vol. 40, no. 2, Feb. 1992, pp. 343-351.

Kyu-Min Kang received the BS, MS, and PhD degrees in electronic and electrical engineering from Pohang University of Science and Technology (POSTECH), Kyungbuk, Korea, in 1997, 1999, and 2003, respectively. Since 2003, he has been with ETRI, Daejeon, Korea. His current research interests include signal processing and digital communications with applications to UWB transmission systems.

Sang-Sung Choi received the BS degree in radio communication from Hanyang University, Korea, in 1977; the ME degree in communication from Korea University, Korea, in 1979; the MS degree in avionics from Ohio University, USA, in 1991; and the PhD degree in electrical engineering from University of Wyoming, USA, in 1999. He is currently a team leader of the IT Convergence Technology Research Laboratory in ETRI, Daejeon, Korea. His main research interests are wireless home networking technologies including UWB technology.